

Katja C. Siegmann  
Tanja Xydeas  
Ralph Sinkus  
Bernhard Kraemer  
Ulrich Vogel  
Claus D. Claussen

## Diagnostic value of MR elastography in addition to contrast-enhanced MR imaging of the breast—initial clinical results

Received: 16 March 2009  
Revised: 14 June 2009  
Accepted: 25 July 2009  
Published online: 1 September 2009  
© European Society of Radiology 2009

K. C. Siegmann (✉) · C. D. Claussen  
Department of Diagnostic  
and Interventional Radiology,  
University Hospital Tuebingen,  
Hoppe-Seyler-Strasse 3,  
72076 Tuebingen, Germany  
e-mail: katja.siegmann@gmx.de  
Tel.: +49-1778265379  
Fax: +49-7071-1295845

T. Xydeas  
Practice of Diagnostic  
and Interventional Radiology,  
Jewish Hospital,  
Heinz-Galinski-Strasse 1,  
Berlin 13347, Germany

R. Sinkus  
Laboratoire Ondes et Acoustique, ESPCI,  
10 rue Vauquelin,  
75005 Paris, France

B. Kraemer  
Department of Obstetrics  
and Gynaecology,  
University Hospital Tuebingen,  
Calwerstrasse 7,  
72076 Tuebingen, Germany

U. Vogel  
Institute of Pathology, University  
Hospital Tuebingen,  
Liebermeisterstrasse 8,  
72076 Tuebingen, Germany

**Abstract Objective:** The purpose of the study was to assess the additional value of magnetic resonance (MR) elastography (MRE) to contrast-enhanced (ce) MR imaging (MRI) for breast lesion characterisation.

**Methods:** Fifty-seven suspected breast lesions in 57 patients (mean age 52.4 years) were examined by ce MRI and MRE. All lesions were classified into BI-RADS categories. Viscoelastic parameters, e.g.  $\alpha 0$  as an indicator of tissue stiffness, were calculated. Histology of the lesions was correlated with BI-RADS and viscoelastic properties. The positive predictive value (PPV) for malignancy, and the sensitivity and specificity of ce MRI were

calculated. Receiver-operating characteristics (ROC) curves were separately calculated for both ce MRI and viscoelastic properties and conjoined to analyse the accuracy of diagnostic performance. **Results:** The lesions (mean size 27.6 mm) were malignant in 64.9% ( $n=37$ ) of cases. The PPV for malignancy was significantly ( $p < 0.0001$ ) dependent on BI-RADS classification. The sensitivity of ce MRI for breast cancer detection was 97.3% (36/37), whereas specificity was 55% (11/20). If ce MRI was combined with  $\alpha 0$ , the diagnostic accuracy could be significantly increased ( $p < 0.05$ ;  $AUC_{ceMRI}=0.93$ ,  $AUC_{combined}=0.96$ ). **Conclusions:** In this study, the combination of MRE and ce MRI could increase the diagnostic performance of breast MRI. Further investigations of larger cohorts and smaller lesions (in particular those only visible on MRI) are necessary to validate these results.

**Keywords** MR elastography · MRI · MRE · Breast · Diagnostic value

### Introduction

Dynamic contrast enhanced (ce) magnetic resonance imaging (MRI) of the breast is the most sensitive imaging technique for breast cancer detection, in particular in premenopausal women and those with dense breasts [1–3]. It can detect cancer that is occult on mammography and

ultrasound [4–6]. The breast imaging reporting and data system (BI-RADS) is used for the diagnostic interpretation of MRI-detected breast lesions [7, 8]. A breast MRI score that can be translated into BI-RADS makes a more detailed analysis of enhancement kinetics and lesion morphology possible [9, 10]. However, there is an overlap of enhancement behaviour and morphology of malignant and benign

lesions [11, 12] that decreases specificity and thereby the diagnostic accuracy of ce MRI.

Breast cancer frequently shows an adjacent desmoplastic stroma reaction in terms of reactive proliferation of connective tissue [13]. This leads to a hardening of the breast tissue, which can be diagnosed by palpation if its extent is large enough. Therefore, clinical breast examination is important for breast cancer detection and it is recommended in addition to mammography in symptomatic patients [14, 15]. However, palpation is user-dependent and diagnostic performance is low, especially in cases of small tumours [16].

Elastography of the breast is a newly developed method that allows an objective analysis of the viscoelastic properties of breast tissues and, therefore, corresponds to an improved and user-independent clinical breast examination that gives measurable physical quantities. There are promising reports on the advantage of ultrasound (US) elastography in the detection and characterisation of breast lesions [17–20]. US elastography is typically restricted to the assessment of one-dimensional (1D) displacement data along the beam line. Thus, compared with full 3D techniques like MRE, it yields inherently more imprecise viscoelastic data. Moreover, it is also restricted to lesions that are visible on US. However, the number of MRI-detected suspicious breast lesions that are not visible on ultrasound is continuously rising because of the increasing use of breast MRI. MR elastography (MRE) of the breast represents a novel imaging technique that is based on the phase-contrast MRI technique [21–24]. It can be used in combination with ce breast MRI and allows imaging of the 3D propagation of low frequency acoustic waves within tissue [21, 25, 26]. As the local properties of the acoustic wave are closely linked to the underlying physical viscoelastic properties of the tissue, it is possible to locally analyse quantitative values of the mechanical properties of tissue such as elasticity and viscosity [24, 27]. Most of the published studies describe MRE of phantoms, pathological specimens, healthy volunteers or of small patient cohorts [21, 22, 24–26, 28]. Prospectively performed analysis of histologically confirmed benign and malignant breast lesions by ce MRI and MRE and the combined assessment of the two techniques have not been published yet.

The two aims of our prospective study were: to correlate viscoelastic properties measured by MRE with histology to evaluate the relationship between the two and to analyse the additional diagnostic value of MRE in differentiating between benign and malignant breast lesions on ce MRI.

## Materials and methods

### Patients

During a 6-month period, consecutive patients who were scheduled for biopsy of a suspicious palpable, mammog-

raphic, ultrasonic or MRI-detected breast lesion were screened for concordance with the inclusion criteria of the study. Approval of the local ethics committee was obtained beforehand, the study design was prospective. Inclusion criteria were a minimum age of 18 years and a lesion size of at least 1 cm to ensure good lesion visibility on ce MRI for targeted MRE. If the patient had no previous ce MRI, the lesion size was measured either on mammography or on ultrasound. In the case of young women (younger than 40 years), mammography was only performed if ultrasound findings suggested a suspicious lesion. Exclusion criteria were contraindications for ce breast MRI, such as claustrophobia, severe obesity, metallic implants, prostheses or clips, cardiac pacemaker, pregnancy and known allergy against paramagnetic contrast media. After detailed explanation of the procedure, written informed consent was given by each patient before breast MRI. All patients had a two-view mammography (Senographe 2000D, GE Healthcare, Chalfont St. Giles, UK) and ultrasound of both breasts (iu22, Philips, Best, The Netherlands) at our institution before breast MRI. Seventy-two women fulfilled the criteria and agreed to participate in the study. Fifteen patients had to be excluded from data analysis. In six cases, MRE could not be finished either because the patient could not lie in the prone position for the entire imaging time ( $n=3$ ) or as a result of technical failures ( $n=3$ ). In three further cases, ce MRI showed no lesion, so that targeted MRE of the supposed lesion was not possible. In six cases, image artefacts that were most likely caused by handling error of the experimental set-up made data analysis impossible. The remaining 57 patients with complete data of ce MRI and MRE of the breast formed the study collective. The mean patient age was 52.4 years, minimum 22 years, maximum 76 years.

### Contrast-enhanced MRI and MRE of the breast

Breast MRI was performed at 1.5 Tesla (Gyrosan Intera, Philips, Best, The Netherlands) with a multi-array double breast coil with integrated mechanical transducers (Fig. 1; Philips Research, Hamburg, Germany) connected to adjustable plates for fixation and compression of both breasts in the cranio-caudal direction. Because strong compression leads to reduced contrast enhancement and to enhanced stiffness of the tissue, the breasts were only mildly compressed in order to obtain good mechanical contact between the pistons and the tissue. Similar pressure was applied for each examination. After a transversely orientated T2-weighted turbo-inversion-recovery sequence, dynamic ce imaging was performed by means of a high-resolution T1-weighted gradient echo sequence [fast field echo (FFE)] in transverse orientation with automated intravenous bolus application of 0.16 mmol of gadopentate dimeglumine (Magnevist; Schering, Berlin, Germany) per kg body weight. One non-enhanced and seven



**Fig. 1** Photograph of the multi-array double breast coil used. Two pairs of transducer pads (*asterisk*) were used for breast fixation and transmission of oscillator-generated mechanical waves into the breast tissue

enhanced series were acquired with an acquisition time of 75 s each and an effective slice thickness of 1.5 mm (TR 8.5 ms, TE 4.2 ms, FOV 380 mm, matrix 512×512). Subtraction images were generated for each contrast-enhanced series by subtraction of the non-enhanced series from the enhanced series.

MRE was planned after identification of the target lesion on ce MRI. The patient remained in the same position as during ce breast MRI so that exact geometrical comparison was possible. Steady-state mechanical waves at 85 Hz were generated and transmitted to the breast tissue via the mechanical set-up. This frequency represented a good compromise between efficient wave penetration deep into the breast tissue (low frequencies) and sufficient spatial resolution (high frequencies). Targeted phase contrast imaging with seven slices of 2 mm in thickness was directed at the centre of the target lesion (TR 495 ms, TE 47 ms, FOV 128 mm, matrix 64×64). Local tissue displacement caused by the propagation of the mechanical waves was measured by a MR phase shift in three dimensions and at eight time points evenly distributed over one period of oscillation. The total time of MRE data acquisition was 12.75 min. Before data analysis, the dynamic phase-shift images of the mechanical waves were visually checked in three dimensions to exclude artefacts. From these data, quantitative values of the complex shear modulus, which represents the viscoelastic properties of the breast tissue (e.g. elasticity and viscosity), were calculated. Technical details about the calculation of shear properties have been previously published [21, 23, 24, 29].

## Data analysis

Evaluation of ce MRI was performed by means of a commercially available workstation (ViewForum, Philips, Best, The Netherlands) by region-of-interest (ROI) analysis and consensus reading of two radiologists with 3 and 5 years' experience of breast MRI. The ROI was set manually and included the most intense pixels (at least five pixels) of the target lesion on early post-contrast subtraction series (first or second ce series). Signal intensity (SI) data of the chosen ROI were displayed and a corresponding SI–time curve was generated automatically (Fig. 2). The maximum diameter of the target lesion was measured and morphological and kinetic lesion characteristics according to the breast MRI score used (Table 1) were assessed. Images of ce MRI were geometrically matched with the reconstructed images of viscoelastic properties so that a corresponding ROI could be placed on the target lesion (Fig. 2). The average values within this ROI were then used to characterise the mechanical properties of each lesion. Histology of the lesions was correlated with the BI-RADS categories corresponding to the respective MRI score [10] and also with the viscoelastic properties. Positive predictive value for malignancy as well as sensitivity and specificity of MRI BI-RADS were calculated. Receiver-operator characteristic (ROC) curves were calculated separately for both ce MRI and viscoelastic properties, and conjoined to analyse the diagnostic performance of ce MRI and MRE alone and combined.

## Histopathology

Sections 5- $\mu$ m thick were cut from formalin-fixed and paraffin-embedded tissues and stained with haematoxylin and eosin according to standardised histopathological techniques. The sections were analysed by an experienced breast pathologist (U.V.), who was unaware of the MRI findings. Breast lesions were classified according to the World Health Organisation classification of tumours of the breast [30]. In line with current guidelines [31], invasive cancers were subdivided according to their nuclear grading (G1–G3). Higher nuclear grading is associated with faster tumour growth and a worse prognosis.

## Statistics

Statistical analyses were performed with MedCalc for Windows 8.2.1.0 (MedCalc, Mariakerke, Belgium) and JUMP 4.0 (JUMP, SAS Institute, USA). The level of significance was defined as  $p < 0.05$ . The sensitivity of ce breast MRI was defined as true-positive cases (BI-RADS 4 and 5) divided by all breast cancers and specificity as true-negative cases (BI-RADS 2 and 3) divided by all benign

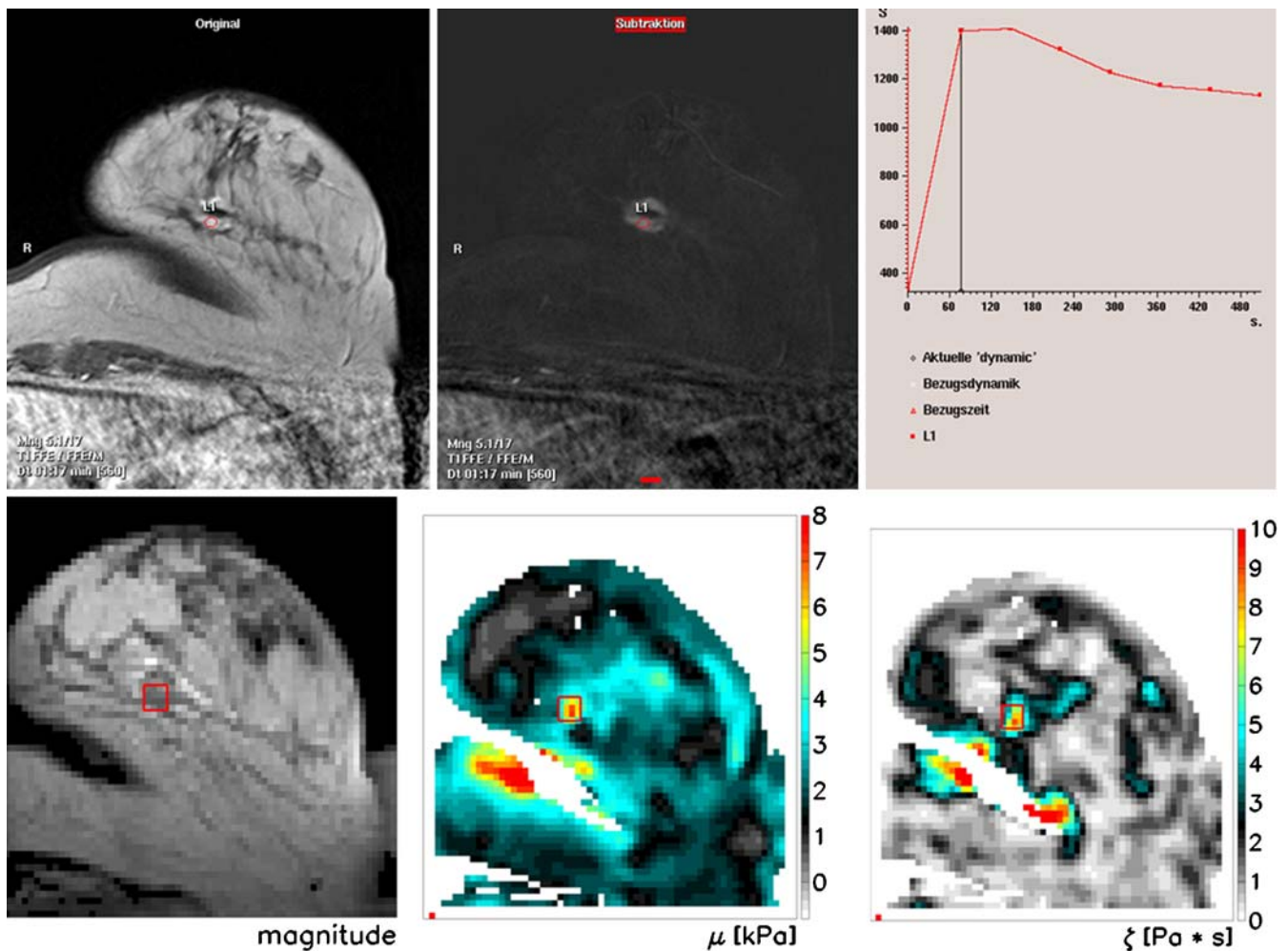


**Fig. 2** Contrast-enhanced (ce) MRI of the left breast shows an enhancing lesion that is analysed by a manually drawn ROI (LI). The upper row shows from left to right: T1-weighted post-contrast image, post-contrast subtraction image and signal intensity–time curve of the chosen ROI, which shows wash-out kinetics. The lesion was assessed to be highly suggestive of malignancy (breast MRI score 7; BI-RADS 5). MRE images of reconstructed viscoelastic

properties were shown in the lower row (left T2-weighted anatomical image = magnitude image, middle elasticity map, right viscosity map). A corresponding ROI of the target lesion was chosen. The lesion showed high values on the elasticity and viscosity maps, which corresponds with very stiff tissue. Histopathology proved this lesion to be an invasive ductal carcinoma of 20 mm in size

lesions. Pearson's chi-squared test was used to test the independence of variables. The area under the curve (AUC) of ROC analysis was used as an estimate of diagnostic accuracy. A pairwise comparison was performed to evaluate differences in the AUC. Differences between malignant and benign lesions with regard to viscoelastic parameters were analysed by *t*-test for independent samples.

## Results

### Patients and lesions

Most patients presented with lesions that were seen on mammography and ultrasound ( $n=37$ ). Sixteen patients

had indeterminate or suspicious ultrasound findings ( $n=16$ ). Lesions that were only detectable by MRI or mammography were present in two cases each. Forty-two lesions (73.7%) were palpable on clinical breast examination. For histological clarification ultrasound-guided, large-core needle biopsy (LCNB; 14 gauge) was performed in 53 cases. Four lesions remained occult after second-look ultrasound: two patients received surgical biopsy after MRI-guided lesion localisation and two patients underwent stereotactic vacuum-assisted biopsy (STVB; 11 gauge) of suspicious microcalcifications.

Thirty-seven lesions (64.9%) were malignant. There were three ductal carcinomas in situ (DCIS) and 34 invasive cancers. Only one invasive carcinoma had a nuclear grading of G1. Most cancers presented a grading of

**Table 1** Breast MRI score for assessment of lesions on contrast-enhanced MRI, modified according to Fischer et al. [9, 10]

Lesion morphology		Points
Shape	Round/oval/lobulated	0
	Irregular (linear, branching, stellate)	1
Margin	Well-defined	0
	Ill-defined	1
Enhancement pattern	Homogeneous	0
	Heterogeneous	1
	Rim enhancement	2
Contrast enhancement kinetics		Points
Initial enhancement <sup>b</sup>	<50%	0
	50–100%	1
	>100%	2
Signal intensity curve <sup>c</sup>	Persistent enhancement	0
	Plateau	1
	Wash-out	2
Total score <sup>a</sup>		0–8

<sup>a</sup>The score can be translated into BI-RADS: lesions with score values of 0–2 points corresponding to BI-RADS 2, score 3 corresponds to BI-RADS 3, score 4–5 means BI-RADS 4 and a score value of 6–8 points means BI-RADS 5

<sup>b</sup>Within the first 3 min after contrast medium injection

<sup>c</sup>Delayed phase from the third minute after contrast medium injection until the last dynamic image

G2 ( $n=30$ ). Three cancers were assessed as G3. The detailed histopathological results are shown in Table 2. Most malignancies were invasive ductal carcinomas ( $n=22$ ). Most benign lesions were based on fibrocystic changes ( $n=8$ ) or fibroadenoma ( $n=7$ ).

### Contrast-enhanced MRI

The mean lesion size on MRI was 27.6 mm ( $\pm 20.5$  mm standard deviation). The positive predictive value (PPV) for malignancy depending on MRI score and corresponding BI-RADS category is shown in Table 3. Because of the small number of patients, BI-RADS 2 and BI-RADS 3 lesions were merged into one group for valid statistical testing. The PPV for malignancy was significantly ( $p<0.0001$ ) dependent on BI-RADS clas-

sification. According to BI-RADS, the PPV for malignancy was 25% (1/4) for BI-RADS 3 and 55.6% (10/18) for BI-RADS 4, as well as 96.3% (26/27) for BI-RADS 5 lesions. The sensitivity of ce MRI for breast cancer detection was 97.3% (36/37), whereas specificity was only 55% (11/20).

### MRE

The parameters Gd and G1 were calculated from MRE data: Gd can be related to the elasticity of the tissue and G1 characterises its viscosity. Both parameters can be converted into another representation, i.e.  $\gamma$  and  $\alpha_0$ , which assume a certain frequency behaviour for the attenuation of tissues [29]. Here,  $\gamma$  characterises tissue with regard to its state of aggregation and varies between

**Table 2** Histological composition of the benign and malignant group of breast lesions (*IDC* invasive ductal carcinoma, *ILC* invasive lobular carcinoma, *DCIS* ductal carcinoma in situ)

Malignant ( $n=37$ )		Benign ( $n=20$ )	
IDC	22	Fibrocystic changes	8
ILC	10	Fibroadenoma	7
Mixed IDLC	1	Sclerosing adenosis	2
DCIS	3	Phylloides tumour	1
Medullary carcinoma	1	Radial scar	1
		Lipoma	1

**Table 3** Distribution of 57 lesions into breast MRI score and BI-RADS categories. The PPV for malignancy is significantly dependent on BI-RADS category (BI-RADS 2 and 3 were analysed as one group)

Breast MRI score	BI-RADS	PPV (no. of lesions)	No. of lesions
1	2	0% (0)*	2
2		0% (0)*	6
3	3	25% (1)*	4
4	4	33.3% (2)	6
5		55.6% (10)*	18
6	5	66.7% (8)	12
7		92.3% (12)	13
8		96.3% (26)*	27
		100% (11)	11
		100% (3)	3
		64.9% (37)	57

\* $p < 0.0001$

the values 0 and 0.5. A value of  $\gamma = 0$  characterises a pure solid state, while a value of  $\gamma = 0.5$  characterises a pure liquid state. The second parameter calculated is  $\alpha_0$ , which reflects the attenuation of the tissue at a frequency of 1 Hz. This value is approximately inversely proportional to the underlying stiffness. Correlation of elasticity (Gd) and viscosity (G<sub>l</sub>) with histology shows that malignant lesions have significantly higher values of both parameters ( $t$ -test:  $p_{Gd} = 0.003$ ;  $p_{G_l} = 0.0002$ ) than benign lesions, which indicate stiffer tissue (Fig. 3). Nevertheless, there is a minor overlap of benign and malignant lesions that is slightly stronger in the case of elasticity than that of viscosity. If  $\gamma$  and  $\alpha_0$  were analysed, malignant lesions would be significantly more liquid ( $\gamma$  near 0.5) and harder

(lower values of  $\alpha_0$ ) than benign lesions (Fig. 4;  $t$ -test:  $p = 0.0001$ ).

#### Combination of ce MRI and MRE

The ROC curves (Fig. 5) demonstrate the diagnostic accuracy of ce MRI alone as well as the performance of  $\gamma$  and  $\alpha_0$  separately and the combined performance of  $\alpha_0$  and ce MRI. Ce MRI and  $\alpha_0$  as indicators of tissue stiffness show similar areas under the curve ( $AUC_{ceMRI} = 0.93$ , 95% CI = 0.83–0.98;  $AUC_{\alpha_0} = 0.88$ , 95% CI = 0.77–0.95), which are not statistically significantly different from each other ( $p = 0.48$ ), whereas the performance of  $\gamma$  is worse ( $AUC_{\gamma} =$

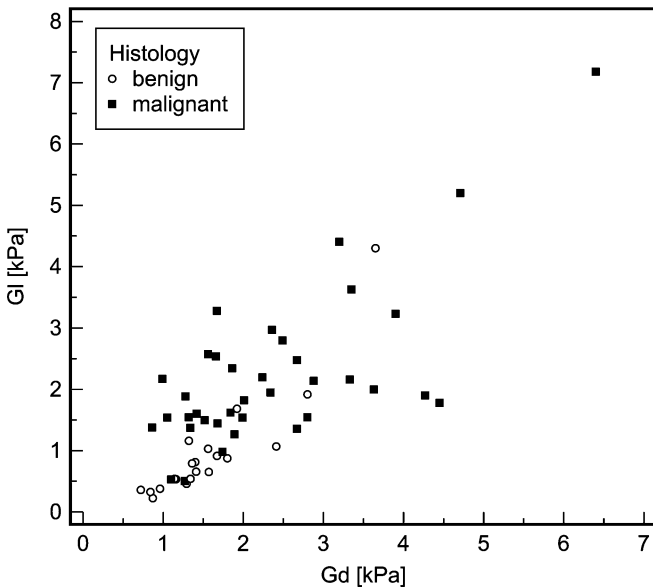


**Fig. 3** Values of elasticity (Gd) and viscosity (G<sub>l</sub>) are significantly different ( $p_{Gd} = 0.003$ ;  $p_{G_l} = 0.0002$ ) in malignant ( $n = 37$ ) and benign ( $n = 20$ ) breast lesions, even if there is a visible overlap of both

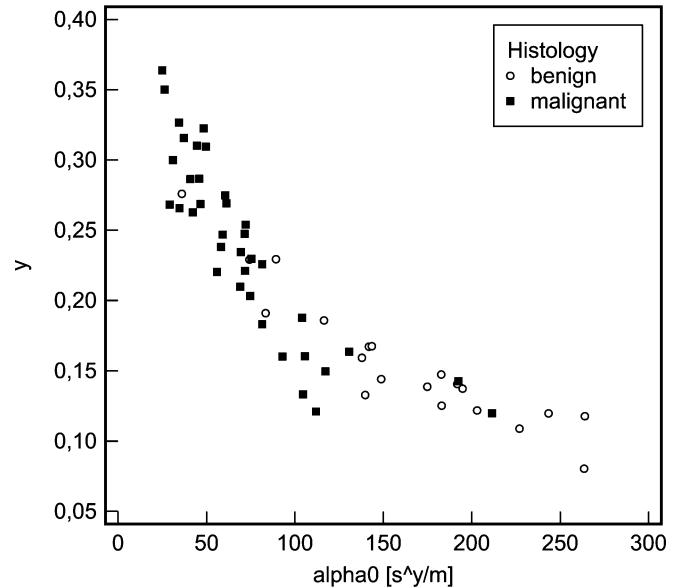


**Fig. 4** Malignant ( $n = 37$ ) and benign ( $n = 20$ ) breast lesions show significantly different values of  $\gamma$  and  $\alpha_0$  ( $p = 0.0001$ ). The unit of  $\alpha_0$  is s <sup>$\gamma$</sup> /m and means: seconds to the power of  $\gamma$  divided by metres

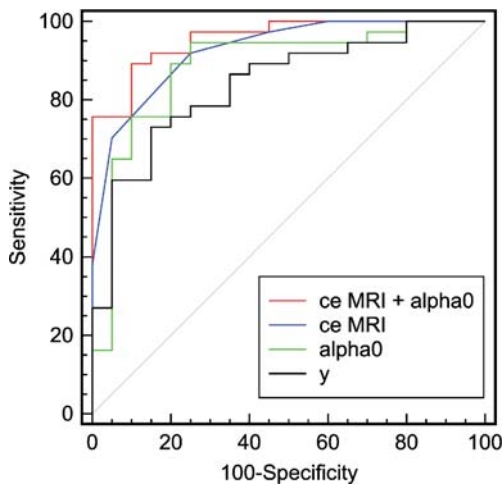


**Fig. 5** ROC curves show diagnostic accuracy of ce MRI and MRE parameters ( $\nu$  and  $\alpha_0$ ) separately as well as the performance of the combination of ce MRI and  $\alpha_0$ . After the combination of ce MRI and  $\alpha_0$  the diagnostic performance could be significantly elevated ( $p=0.03$ )

0.84, 95% CI=0.72–0.92). The combination of ce MRI and  $\alpha_0$  can elevate the diagnostic accuracy of breast MRI significantly compared with ce MRI alone ( $p=0.03$ ;  $AUC_{\text{combined}}=0.96$ , 95% CI=0.87–0.99). In this way the specificity of breast MRI could be elevated from 75% to 90% at a persistently high sensitivity of 90%.

## Discussion

In this study ce breast MRI with assessment of MRI score and corresponding BI-RADS categorisation gives high diagnostic accuracy with an AUC value of 0.93. However, the specificity of ce MRI remains moderate (55%) whereas sensitivity is high (97.3%). This corresponds with published studies [1, 3] and demonstrates that breast cancer detection is already excellent, but specificity is still an important issue. Breast MRE is a non-invasive approach to improving the differentiation of benign and malignant enhancing lesions by analysis of their viscoelastic properties, which reveal information regarding their architecture. In particular,  $\alpha_0$  as expression of the hardness of the tissue seemed to be a valuable diagnostic parameter. In this study, viscoelastic information could significantly elevate the specificity and thereby the diagnostic accuracy of breast MRI, whereby breast cancers had higher values of elasticity and viscosity than benign lesions. There are very few in vivo studies of breast MRE. Lorenzen et al. [32] analysed 20 patients by MRE and found significantly elevated values of elasticity in 15 breast cancers with a mean tumour size of 32 mm. Sinkus et al. performed MRE in 15 patients [23] and found good separation between six cancers and six fibroadenomas because of their different

shear modulus. However, similar to the results of our study, there is an overlap of elasticity values of malignant and benign lesions [32]. Therefore, they concluded that breast cancer diagnosis by MRE alone would be not advisable. Xydeas et al. [33] report 16 patients in whom SI data and viscoelastic lesion properties were compared and showed good correspondence, but no statistical test could be used because of the small patient population. Sinkus et al. [29] could demonstrate a significant diagnostic gain in 68 breast lesions if the MRE variable  $\delta$  has been used.

In our study set-up, only one target lesion could be analysed by each MRE (seven slices, 2-mm slice thickness). Further investigations aimed at whole breast technique-independent 3D elastography would make MRE analysis of any desired lesion together with analysis of ce MRI possible in one step. First results have shown elasticity values that are reasonably close to true values [34], but clinical evaluation of this method is yet to be performed.

Implementation of MRE into clinical routine has not yet been established. Only if MRE software is integrated into MR software and workstations can routine use of MRE be practicable within a reasonable time. Moreover, faster imaging protocols for MRE are necessary to prevent imaging abort because of patient discomfort. However, faster imaging technique necessitates TSE or EPI sequences, which are accident sensitive. Therefore, we did not use those techniques. But one recently published paper reports rapid MRE using gel phantoms with a 1D technique, which offers stiffness estimates comparable to those with 3D MRE [35]. Whether this technique would be adequate for in vivo MRE has not yet been investigated.

The study has certain limitations. First, the number of benign lesions was rather low ( $n=20$ ) because of the refusal of patients without highly suspicious lesions, after receiving information about the necessity of using contrast agent application for ce MRI, to take part in the study. Second, the lesions studied were often large (mean size 27.6 mm) and palpable because of the inclusion criteria. However, difficulties in lesion classification usually occur in cases of small lesions that are only visible on MRI, because mammographic and ultrasound-detected suspicious lesions can be easily clarified by LCNB or STVB. Nevertheless, this study had only a small number of lesions only detected on MRI ( $n=2$ ). Third, the patient cohort was quite small ( $n=57$ ), so that only preliminary conclusions could be drawn.

In conclusion, this study shows that MRE may possibly provide additional valuable diagnostic information to elevate the specificity and thereby the accuracy of ce breast MRI. Further investigations of larger prospective cohorts with smaller and in particular lesions only visible on MRI are necessary to validate the diagnostic benefit of MRE in addition to ce MRI.

## References

1. Stomper PC, Winston JS, Herman S et al (1997) Angiogenesis and dynamic MR imaging gadolinium enhancement of malignant and benign breast lesions. *Breast Cancer Res Treat* 45:39–46
2. Morris EA (2002) Breast cancer imaging with MRI. *Radiol Clin North Am* 40:443–466
3. Kuhl C (2007) The current status of breast MR Imaging. Part I. Choice of technique, image interpretation, diagnostic accuracy, and transfer to clinical practice. *Radiology* 244:356–378
4. Morris EA, Liberman L, Ballon DJ et al (2003) MRI of occult breast carcinoma in a high-risk population. *AJR Am J Roentgenol* 181:619–626
5. Deurloo E, Muller SH, Peterse JL (2005) Clinically and mammographically occult breast lesions on MR Images: potential effect of computerized assessment of clinical reading. *Radiology* 234:693–701
6. Van Goethem M, Schelfout K, Dijckmans L et al (2004) MR mammography in the pre-operative staging of breast cancer in patients with dense breast tissue: comparison with mammography and ultrasound. *Eur Radiol* 14:809–816
7. American College of Radiology (ACR) (2003) Breast imaging reporting and data system (BI-RADS) atlas, 3rd edn. American College of Radiology, Reston
8. Mann RM, Kuhl CK, Kinkel K et al (2008) Breast MRI: guidelines from the European Society of Breast Imaging. *Eur Radiol* 18:1307–1308
9. Fischer U, Kopka L, Grabbe E (1999) Breast carcinoma: effect of preoperative contrast-enhanced MR imaging on the therapeutic approach. *Radiology* 213:881–888
10. Baum F, Fischer U, Vosschenrich R et al (2002) Classification of hypervascularized lesions in CE MR imaging of the breast. *Eur Radiol* 12:1087–1092
11. Kuhl CK, Schild HH (2000) Dynamic image interpretation of MRI of the breast. *J Magn Reson Imaging* 12:965–974
12. Siegmann KC, Mueller-Schimpfle M, Schick F et al (2002) MR imaging-detected breast lesions: histopathologic correlation of lesion characteristics and signal intensity data. *AJR Am J Roentgenol* 178:1403–1409
13. Meng L, Zhou J, Sasano H et al (2001) Tumor necrosis factor alpha and interleukin 11 secreted by malignant breast epithelial cells inhibit adipocyte differentiation by selectively down-regulating CCAAT/enhancer binding protein alpha and peroxisome proliferator-activated receptor gamma: mechanism of desmoplastic reaction. *Cancer Res* 61:2250–2055
14. Saslow D, Hannan J, Osuch J et al (2004) Clinical breast examination: practical recommendations for optimizing performance and reporting. *Cancer J Clin* 54:327–344
15. Feigin KN, Keating DM, Telford PM et al (2006) Clinical breast examination in a comprehensive breast cancer screening program: contribution and cost. *Radiology* 240:650–655
16. Bancej C, Decker K, Chiarelli A et al (2003) Contribution of clinical breast examination to mammography screening in the early detection of breast cancer. *J Med Screen* 10:16–21
17. Tan SM, The HS, Mancier JF et al (2007) Improving B mode ultrasound evaluation of breast lesions with real-time ultrasound elastography—a clinical approach. *Breast* 17:252–257
18. Tohno E, Ueno E (2008) Current improvements in breast ultrasound, with a special focus on elastography. *Breast Cancer* 15:200–204
19. Zhu QL, Jiang XY, Liu JB et al (2008) Real-time ultrasound elastography: its potential role in assessment of breast lesions. *Ultrasound Med Biol* 34:1232–1238
20. Itoh A, Ueno E, Tohno E et al (2006) Breast disease: clinical application of US elastography for diagnosis. *Radiology* 239:341–350
21. Sinkus R, Lorenzen J, Schrader D et al (2000) High-resolution tensor MR elastography for breast tumour detection. *Phys Med Biol* 45:1649–1664
22. Von Houten EEW, Doyley MM, Kennedy FE (2003) Initial in vivo experience with steady-state subzone-based MR elastography of the human breast. *J Magn Reson Imaging* 17:72–85
23. Sinkus R, Tanter M, Xydeas T et al (2005) Viscoelastic shear properties of in vivo breast lesions measured by MR elastography. *Magn Reson Imaging* 23:159–165
24. Sinkus R, Tanter M, Catheline S et al (2005) Imaging anisotropic and viscous properties of breast tissue by magnetic resonance-elastography. *Magn Reson Med* 53:372–387
25. Plewes DB, Bishop J, Samani A et al (2000) Visualization and quantification of breast cancer biomechanical properties with magnetic resonance elastography. *Phys Med Biol* 45:1591–1610
26. McKnight AL, Kugel JL, Rossmann PJ et al (2002) MR elastography of breast cancer: preliminary results. *AJR Am J Roentgenol* 178:1411–1417
27. Sinkus R, Tanter M, Bercoff J et al (2008) Potential of MRI and Ultrasound Radiation Force in Elastography: Applications to Diagnosis and Therapy. *Proc IEEE* 96:490–499
28. Lorenzen J, Sinkus R, Biesterfeldt M et al (2003) Menstrual-cycle dependence of breast parenchyma elasticity: estimation with magnetic resonance elastography of breast tissue during the menstrual cycle. *Invest Radiol* 38:236–240
29. Sinkus R, Siegmann K, Xydeas T et al (2007) MR elastography of breast lesions: understanding the solid/liquid duality can improve the specificity of contrast-enhanced MR mammography. *Magn Reson Med* 58:1135–1144
30. Tavassoli FA, Devillee P (2006) World health organization classification of tumors. Pathology and genetics. Tumours of the breast and female genital organs. IARC Press Lyon
31. Pery N, Broeders M, de Wolf C et al (2006) European commission: European guidelines for quality assurance in breast cancer screening and diagnosis, 4th edn. Office of Official Publications of the European Communities, Luxembourg
32. Lorenzen J, Sinkus R, Lorenzen M et al (2002) MR elastography of the breast: preliminary clinical results. *Rofo* 174:830–834
33. Xydeas T, Siegmann KC, Sinkus R et al (2005) Magnetic resonance elastography of the breast—correlation of signal intensity data and viscoelastic properties. *Invest Radiol* 40:412–420
34. Ou JJ, Ong RE, Yankeelov TE et al (2008) Evaluation of 3D modality-independent elastography for breast imaging: a simulation study. *Phys Med Biol* 53:147–163
35. Glaser KJ, Felmlee JP, Ehman RL (2006) Rapid MR elastography using selective excitations. *Magn Reson Med* 55:1381–1389